Kidney International, Vol. 62 (2002), pp. 1338–1348

Protective role of nitric oxide in mice with Shiga toxin-induced hemolytic uremic syndrome

GRACIELA I. DRAN, GABRIELA C. FERNÁNDEZ, CAROLINA J. RUBEL, EMILSE BERMEJO, SONIA GOMEZ, ROBERTO MEISS, MARTÍN A. ISTURIZ, and MARINA S. PALERMO

División Medicina Experimental, División Inmunología, and Departamento de Hemostasia y Trombosis, Instituto de Investigaciones Hematológicas, and Departamento de Patología, Centro de Estudios Oncológicos, Academia Nacional de Medicina, Buenos Aires, Argentina

Protective role of nitric oxide in mice with Shiga toxin-induced hemolytic uremic syndrome.

Background. Nitric oxide (NO) is an endogenous vasodilator and platelet inhibitor. An enhanced NO production has been detected in patients with hemolytic uremic syndrome (HUS), although its implication in HUS pathogenesis has not been clarified.

Methods. A mouse model of Shiga toxin 2 (Stx2)-induced HUS was used to study the role of NO in the development of the disease. Modulation of L-arginine-NO pathway was achieved by oral administration of NO synthase (NOS) substrate or inhibitors, and renal damage, mortality and platelet activity were evaluated. The involvement of platelets was studied by means of a specific anti-platelet antibody.

Results. Inhibition of NO generation by the NOS inhibitor L-NAME enhanced Stx2-mediated renal damage and lethality; this effect was prevented by the addition of L-arginine. The worsening effect of L-NAME involved enhanced Stx2-mediated platelet activation, and it was completely prevented by platelet depletion.

Conclusions. NO exerts a protective role in the early pathogenesis of HUS, and its inhibition potentiates renal damage and mortality through a mechanism involving enhanced platelet activation.

Hemolytic uremic syndrome (HUS) is characterized by hemorrhagic diarrhea followed by microangiopathic hemolytic anemia, thrombocytopenia and acute renal failure. Shiga toxin (Stx) producing *Escherichia coli* has been strongly associated with outbreaks of the disease [1]. The toxin binds to a globotriaosil ceramide (Gb3) receptor and interferes with protein synthesis, mainly on capillary endothelial cells. In addition, the injured endothelium loses its anti-thrombogenic properties, thus leading to a pathological cascade that may involve the production of nitric oxide (NO), prostacyclin (PGI_2), platelet-activating factor (PAF), von Willebrand factor and interleukins (ILs) [2, 3]. In humans, the kidney is the primary target, probably due to high basal level of Gb3. The typical renal histologic finding is a characteristic glomerular thrombotic microangiopathy (TMA); the glomerulus appears wrinkled, with endothelial cell swelling and capillary wall thickening, and the lumen of the capillaries is largely obstructed by fibrin thrombi [2, 4]. A characteristic pattern of impaired platelet function is found in most patients with HUS. This impairment consists in thrombocytopenia, shortened survival of remaining circulating platelets, abnormal response to aggregating agents, platelet exhaustion and pathological platelet microthrombi found in the kidney [2, 5–8], and it is thought to be a consequence of previous endothelial damage-induced platelet activation, since the platelet content of specific granules is markedly reduced [6, 8].

Nitric oxide is an endogenously produced vasodilator, the cellular effects of which are signaled via stimulation of 3′,5′-guanosine monophosphate (cGMP) [9]. NO is also a well known inhibitor of platelet function. Among its effects, inhibition of platelet aggregation and adhesion to damaged endothelium as well as inhibition of P-selectin expression and fibrinogen binding to platelets have been described [10, 11]. There are several clinical studies on the enhanced NO production in patients during the active phase of HUS [12–14]; however, its role in the pathogenesis of the syndrome has not yet been assessed, and whether it exerts a protective or a detrimental effect remains controversial. Due to its anti-thrombogenic properties, it has been hypothesized that treatment with oral L-arginine, the physiological precursor of NO, could provide an alternative clinical approach to the control of HUS [15]. On the other hand, NO is a potent cytotoxic agent that could mediate vascular injury. Thus, an up-regulation of NO production could enhance vessel wall damage and vascular dysfunction [13, 16–18].

Key words: pathogenesis of HUS, hemorrhagic diarrhea, platelet activation, thrombocytopenia, acute renal failure.

Received for publication August 28, 2001
and in revised form March 29, 2002
Accepted for publication May 1, 2002

The Stx-treated mouse is a widely used model to study the clinical and histopathological changes associated with human HUS, in which gastrointestinal, neurologic and systemic symptoms have been reproduced [19–25]. In the mouse kidney, histological damage has been documented as taking place mainly in renal tubules and to a lesser degree in glomeruli. The toxin produces severe acute renal cortical tubular necrosis [19–25] and glomerular mesangial proliferation and fibrinogen deposition as well as vascular congestion and interstitial inflammation [25]. However, to date no glomerular thrombotic lesions characteristic of human HUS have been noticed in mice [25].

In this study we have used an HUS model of Stx2-injected mice [26, 27] to determine the role of endogenously synthesized NO in the pathology of the syndrome. We demonstrate that Stx2-induced renal toxicity and mortality are markedly enhanced by inhibition of the endogenous NO production. The underlying mechanism involves increased platelet activity and thrombus formation.

METHODS

Mice

BALB/c mice were bred in the animal facility at the Departamento de Medicina Experimental, Academia Nacional de Medicina, Buenos Aires. Male mice aged 8 to 16 weeks and weighing 20 to 24 g were used throughout the experiments. They were maintained under a 12-hour light/dark cycle at a temperature of 22 ± 2°C and fed with standard diet and water ad libitum. The experiments performed herein were conducted according to principles set forth in the Guide for the Care and Use of Laboratory Animals (National Institute of Health, 1985).

Stx2 preparation

Stx2 was kindly provided by Dr. Sugiyama Junichi from Denka Seiken Co., Ltd. (Nigata, Japan). Purity was analyzed by the supplier showing only one peak in high pressure liquid chromatography (HPLC). Stx2 preparation was checked for endotoxin contamination by the *Limulus amoebocyte* lysate assay given that 1 IU/mL is equal to 0.1 ng/mL of United States Pharmacopea standard *E. coli* endotoxin. Stx2 preparation contained less that 40 pg lipopolysaccharide (LPS)/μg of Shiga toxin protein. Stx2 was tested for cytotoxic activity on Vero cells as previously described [28] in the Instituto Nacional de Enfermedades Infecciosas, ANLIS "Dr. C.G. Malbrán," Buenos Aires, Argentina. Briefly, Vero cells were grown in Eagle's minimum essential medium with Earle salts and non-essential amino acids (Gibco Diagnostics, Madison, WI, USA) supplemented with 7% fetal calf serum (FCS; Sigma Chemical Co., St. Louis, MO, USA), 0.03 mol/L glutamine, 50 μg/mL gentamicin and 2.5 μg/mL fungizone in microtiter plates (Nunc, Intermed, Roskilde, Denmark). Aliquots (50 μL) of serial two-fold dilutions of the samples containing Stx2 were added to each well (25,000 Vero cells) and incubated for three days at 37°C in 5% CO_2. Vero cells were daily examined for cytotoxicity. The 50% cytotoxic dose (CD_{50}) corresponded to the dilution required to kill 50% of the Vero cells: CD_{50} was ~0.063 pg.

Stx2 treatment

Mice were intravenously injected with a dose of Stx2 required to kill 50% of mice (LD_{50}). Our previous study evaluated the in vivo lethality of Stx2 by serial dilutions in pyrogen-free saline [26]. The LD_{50} was approximately 2.5×10^{-5} mg/kg body weight (500 pg/mouse), for which the mean time of death was 3.5 days. The same batch of Stx2 preparation was used throughout the experiments.

NO synthase (NOS) modulation

In all protocols, solutions of the NOS inhibitors N^G-nitro-L-arginine methyl ester (L-NAME; Sigma Chemical Co.), L-N^6-(1-imino-ethyl)-lysine (L-NIL; Calbiochem-Novabiochem Corp., San Diego, CA, USA), and aminoguanidine (AG; Sigma), the D-form of L-NAME (D-NAME; Sigma) and the physiological substrate for the enzyme L-arginine (L-ARG; Sigma) were freshly prepared every two days, administered via the drinking water and consumed ad libitum. The final concentrations used were: L-NAME and D-NAME, 1 mg/mL; L-NIL, 10 mmol/L; AG, 100 μg/mL; L-ARG, 10 mg/mL. Treatments began 24 hours prior to the injection of Stx2 and lasted until the end of the experiments, inducing no detectable variations in the NOS activity as assessed by NO production herein and in previous reports. Similarly, these treatments did not influence water or food intake or impair weight gain in naive mice [29–32].

Nitric oxide assay

The concentration of the anions NO_2^- and NO_3^- in plasma was used as a quantitative measure of NO production. A commercially available kit for total NO determination (R & D Systems, Inc., Minneapolis, MN, USA) was employed. Briefly, the assay determined total NO based on the enzymatic conversion of nitrate to nitrite by nitrate reductase. The reaction was followed by the colorimetric detection at 540 nm of the azo dye product of the Griess reaction (50 μL samples plus an equal volume of Griess reagent consisting of 1% sulfanilamide, 0.1% naphthylethylene diamine dihydrochloride, and 2.5% H_3PO_4).

Plasmatic urea determination

Blood was obtained by puncture of the retroorbital plexus. Biochemical determinations of urea in serum were performed in an autoanalyzer CCX Spectrum (Abbott Diagnostics System, Buenos Aires, Argentina) following standardized instructions.

Histological studies

Animals from the control and experimental groups were sacrificed 72 hours after Stx2 injection and subjected to necropsy. Both kidneys from each mouse (8 per group) were longitudinally bisected and fixed in 10% neutral formalin and routinely processed. Sections of paraffin-embedded tissue were stained with hematoxylin and eosin (H&E) and periodic acid-Schiff (PAS) and examined by light microscopy. Glomerular injury was evaluated by the presence of hypercellularity, crescent formation and thrombosis. Tubular injury was evaluated by the presence of alterations in tubular epithelium, basement membrane integrity and necrosis. Vascular interstitial congestion also was assessed.

Immunostaining for fibrinogen

Another set of kidney sections was stained for fibrinogen using an immunoperoxidase method. Endogenous peroxidase was blocked with 0.5% hydrogen peroxide in methanol. Sections were then exposed to rabbit anti-human fibrinogen, which cross-reacts with mouse fibrinogen (Dako Corp., Carpinteria, CA, USA) at 1:50. For detection, a commercial kit (Dako LSAB 2-System HRP-DAB) was employed. Counterstaining was done with hematoxylin. Glomeruli showing thrombi by fibrinogen staining were counted and expressed as percentage (N = 100 40× magnification fields).

Platelet aggregation studies

Blood samples were obtained from each mouse by retro-orbital punction. Nine volumes of whole blood were gently mixed in a polyethylene tube with one volume of a 3.8% (wt/vol) trisodiun citrate solution in water. Platelet-poor plasma (PPP) was prepared by centrifugation of the blood at 1000 × g for 20 minutes at 4°C, and platelet-rich plasma (PRP) was obtained by centrifugation of the blood at 300 × g for 20 minutes at room temperature. For more accurate comparison, PRPs from control and experimental groups were adjusted with autologous PPPs to achieve comparable platelet counts. Aggregation studies were performed using a Chrono-log whole blood lumi-aggregometer [Ca2]. Briefly, 450 μL of PRP were added with a stirring bar to a glass cuvette and were allowed to warm at 37°C prior to the addition of the agonists. Light transmission was adjusted to 10% for PRPs and to 90% for PPPs. At time zero, the aggregating agents were added in 50 μL volumes. Platelet aggregation resulted in an increased light transmission and upward deflection of the recording curve. Adenosine diphosphate (ADP) and arachidonic acid (AA) were purchased from Sigma. ADP and AA were dissolved in saline to a final concentration of 2.5μmol/L and 0.5 mmol/L, respectively.

Flow cytometry studies

Mepacrine staining was detected as previously outlined [33]. Briefly, PRP was incubated at 3°C in the dark for 30 minutes in 0.1 mmol/L quinaqcrine mustard (mepacrine; Sigma) and then washed twice in CGS buffer (0.109 mol/L trisodium citrate, 30 mmol/L glucose, 0.15 mol/L sodium chloride). For each sample a second aliquot of platelets was simultaneously incubated without stain and used as a negative control. Mepacrine-loaded platelets were resuspended in CGS buffer to a concentration of 200 × 10^5 cells/L for flow cytometry, and kept in the dark until analyzed. A Beckton Dickinson FACScan configured for FITC emission at a range of 520 to 530 nm was used to detect the mepacrine. The platelet population was gated by the distinct pattern on the histogram of log forward scatter versus log side scatter. An analysis region was set from log 1 of the fluorescence scale, and percentages of mepacrine-positive gated cells were compared.

Platelet depletion studies

Platelet rich plasma from control BALB/c mice were obtained as stated above and washed twice. Adult rabbits were injected IV with a suspension of 1 × 10^9 platelets per dose at days 1, 10, 20 and 30. At day 40, animals were bled by puncture of the ear vein and serum was maintained at −20°C. Rabbits were boosted monthly. In preliminary experiments we determined that an IP injection of 100 μL of a 1:2 dilution of the antiserum induced an almost complete depletion of mice platelets four hours after the injection (N° platelets × 10^3/μL, 899 ± 15 for control and 7 ± 0.2 for treated mice). Similar platelet depletion was maintained throughout the experiments by a first injection of the antiserum four hours before Stx2 administration and successive injections every 12 hours.

Statistical analysis

All data correspond to the mean ± SEM of individual mice. Statistical differences were determined using the one-way analysis of variance (ANOVA), and $P < 0.05$ was considered significant. Individual groups were compared using the unpaired Student t test. Significance in survival experiments was evaluated by the Fisher exact test.

RESULTS

Effect of NO modulation on Stx2-induced lethality

The effect of NO modulation on Stx2 toxicity was evaluated through mortality rates. Groups of six mice were treated orally with NOS inhibitors or substrate, and 24 hours later were injected intravenously with 500 pg/mouse (LD_{50}) of purified Stx2. Survival data shown in Figure 1A indicate that pretreatment of mice with L-NAME enhanced the lethal toxicity of Stx2. The mean

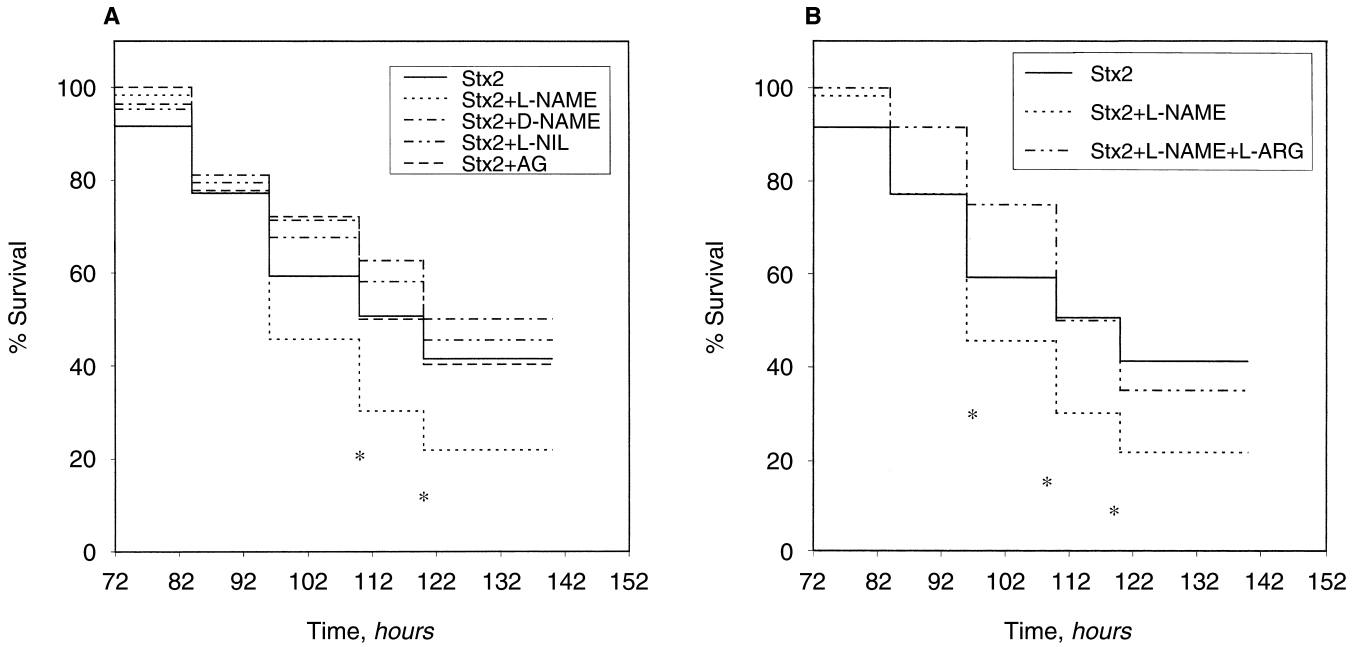

Fig. 1. Effect of nitric oxide (NO) modulation on Shiga toxin 2 (Stx2)-induced lethality. (*A*) Effect of L-NAME modulation upon Stx2-induced lethality. Groups of six mice were treated with nothing, L-NAME, D-NAME, L-NIL or AG from time −24 hours until the end of the experiment. At time 0, mice were intravenously injected with 500 pg of Stx2; time of death was evaluated up to 150 hours after Stx2 injection. Pooled survival percentages corresponding to seven separate experiments are shown. (*$P < 0.01$, compared to Stx2). (*B*) Reversibility of L-NAME–induced increment in Stx2-mediated mortality by the NOS substrate, L-ARG (*$P < 0.05$, compared to Stx2+L-NAME+L-ARG, $N = 10$).

time to death (± SEM) for Stx2 and Stx2+L-NAME-treated mice was 121.9 ± 5.2 and 91.2 ± 2.1 hours, respectively ($P < 0.01$). The mortality rate for mice treated with Stx2 plus the inactive enantiomer D-NAME did not differ from that of Stx2-treated mice. On the other hand, administration of aminoguanidine (AG) or L-NIL, both selective inducible NOS (iNOS) inhibitors, did not affect Stx2 toxicity. We next determined the effect of the physiological substrate of NOS, L-ARG. As shown in Figure 1B, L-ARG was able to prevent L-NAME-mediated potentiation of Stx2 toxicity when administered together; L-ARG alone, however, exerted no significant effect (data not shown).

Urea levels in plasma

Our previous report on mice inoculated with one LD_{50} of Stx2 showed an increase in plasmatic urea at 72 hours after injection, consistent with renal damage [26]. To ascertain whether NOS inhibition enhanced Stx2 toxicity by increasing its specific renal damage, animals from the different groups were bled at 48, 72 and 96 hours post-Stx2 injection, and the level of plasmatic urea was determined. As shown in Figure 2, all Stx2-treated mice displayed abnormal renal function, evidenced by elevated uremia (range 86 to 380 mg%), compared to controls (range 47 to 54 mg%). The L-NAME pretreated animals displayed significantly higher urea levels at 72 and 96 hours, compared to the Stx2 group, which were consistent with the above mentioned increment in mortality

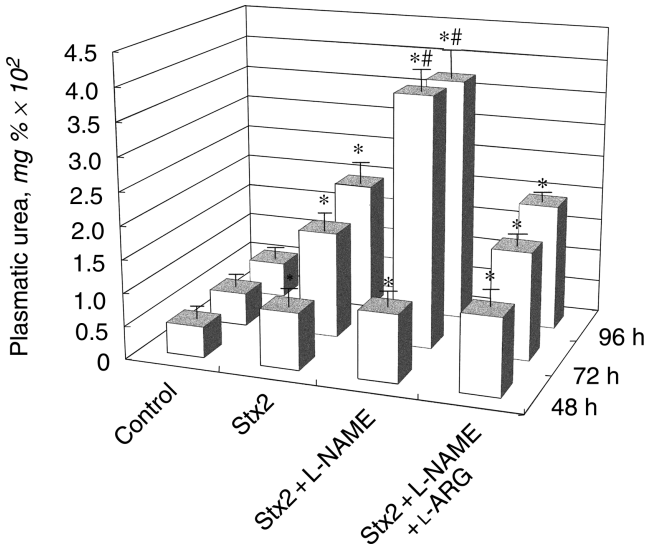

Fig. 2. Plasmatic urea variation induced by Stx2 and L-NAME. Mice were bled at different times after Stx2 injection. Data are from one representative experiment out of five, and show mean ± SEM of plasmatic urea values from 10 mice/group (*$P < 0.01$, compared to controls; #$P < 0.01$, compared to Stx2, to L-NAME and to Stx2+L-NAME+L-ARG).

rates. Since it is well known that chronic administration with L-NAME can modify renal function, we also measured urea in plasma of mice given only L-NAME (range 39 to 58%), and detected no differences compared to the control group. Again, when administered together

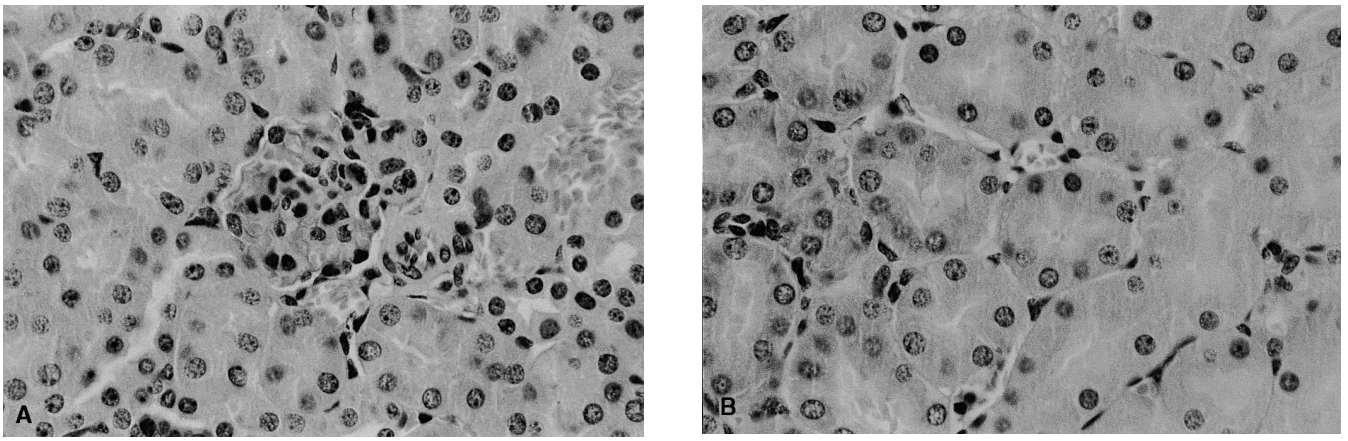

Fig. 3. Histology of kidneys from Stx2-treated animals (H&E, PAS staining). (*A*) Renal cortical tissue showing mild glomerular mesangial hypercellularity and crescent formation. Glomerular capillaries with mild incipient thrombus formation (×400). (*B*) Cortical tubular epithelial cell swelling. Tubular cells with loss of apical microvilli and tubular basement membrane shrinkage (×400).

with L-NAME, L-ARG was able to prevent the L-NAME-mediated potentiation of Stx2-induced renal toxicity. It can be postulated that the inhibition of NO production enhanced Stx2-induced mortality by potentiating renal injury.

Histological examination

The H&E and PAS stainings revealed in the Stx2 group a moderate to severe widespread glomerular mesangial hypercellularity and crescent formation (Fig. 3A) with tubular epithelial swelling and disrupted basement membrane in proximal cortex (Fig. 3B). In the Stx2+ L-NAME group, glomerular thrombosis was diffusely distributed throughout the cortex (Fig. 4A). A detail shows a glomerulus with deposits of hyaline, PAS-positive amorphous material in the glomerular tufts (Fig. 4B), consistent with capillary thrombosis [34, 35]. Severe tubular epithelial cell damage with loss of basement membrane occurred in proximal and distal tubules of the cortex, leading to widespread necrosis (Fig. 4 A, C, D). Kidneys corresponding to the Stx2+L-NAME+L-ARG group showed a lesser degree of renal damage; there were dilated glomerular capillaries with incipient hyaline amorphous deposits, and no evidence of epithelial cell necrosis in tubules (data not shown).

Kidneys from mice treated only with L-NAME showed significant dilated glomerular capillaries and interstitial vascular congestion, which probably reflect the hemodynamic changes associated to the vasoconstrictor effect of L-NAME. In this group epithelial cells in nephron segments were normal in appearance (data not shown). Kidneys from control mice lacked histological changes (data not shown).

Immunostaining for fibrinogen

The presence of thrombi inside glomerular capillaries was assessed by a specific staining for fibrinogen. Figure 5A shows the percentage of compromised glomeruli for every experimental group. In mice treated with Stx2 almost half of the glomeruli were affected; fibrinogen deposition appeared either adhered to the vessel wall or occluding the lumen (Fig. 5B). A marked increase in the thrombosis phenomenon was seen in the Stx2+ L-NAME group, where almost every glomerulus presented fibrinogen deposition in the same pattern described above (Fig. 5C). L-ARG, administered along with L-NAME, induced a degree of thrombosis similar to that observed in the Stx2-treated group, thus preventing the effect of L-NAME (data not shown). In all groups thrombosis was not confined to glomerular microcirculation, but occasionally extended to interstitial capillaries. Neither control nor L-NAME-treated mice showed any sign of thrombosis (data not shown).

Stx2 and L-NAME effects on platelet activation

Increased platelet activity and thrombus formation would account for Stx-induced renal damage in patients with HUS. Since NO is an active platelet inhibitor, we evaluated the possibility that inhibition of its synthesis could potentiate Stx2-mediated lethality by enhancing platelet activation. Table 1 summarizes platelet counts of control and experimental animals at 12 and 24 hours after Stx2 injection. At an early period (12 hours), the platelet number was elevated in the Stx2-treated group, and L-NAME significantly enhanced this effect. At 24 hours, however, both Stx2 and Stx2+L-NAME-treated mice showed thrombocytopenia, which persisted up to 72 hours. To study the functional status of platelets, aggregation studies were performed. We assayed currently used platelet agonists such as arachidonic acid (AA) and ADP, which induced a rapid aggregative response. Percentages of aggregation against AA are shown in Figure 6A. Platelets from Stx2-treated animals were acti-

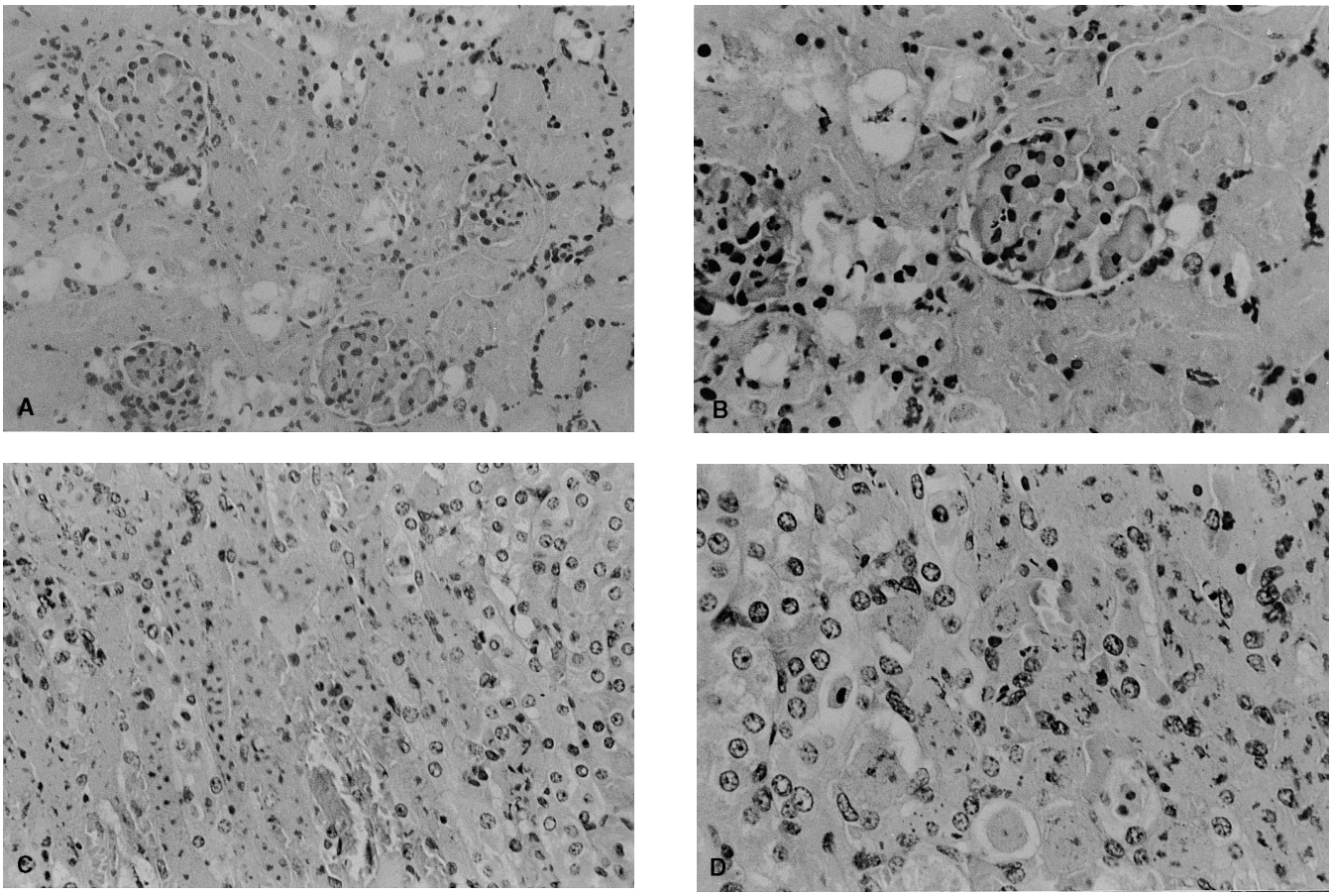

Fig. 4. Histology of kidneys from Stx2+L-NAME-treated animals (H&E, PAS staining). (*A*) Cortical renal tissue with glomeruli and proximal cortical tubules showing a widespread severe damage (×250). (*B*) Glomeruli with hypercellularity, crescent formation and evident capillary thrombosis, surrounded by cortical tubules with acute epithelium necrosis (×400). (*C*) Distal cortical tubules with severe necrosis of tubular epithelium and dilated interstitial capillaries (×250). (*D*) Loss of tubular architecture due to severe and broad necrosis (×400).

vated at 24 hours post-Stx2 injection, while in Stx2+ L-NAME-treated mice activation was achieved earlier (12 hours). This activation was followed by an inhibited response in both groups, probably reflecting platelet exhaustion. A similar pattern was observed when ADP was used as agonist (Fig. 6B). Platelets from Stx2− and Stx2+L-NAME-treated animals were clearly activated at 24 hours. This activation resulted in inhibition at 48 and 72 hours in both groups, although inhibition in Stx2+ L-NAME group was markedly higher. Taken together, these results suggest that Stx2 treatment elicited platelet activation, which was rapidly followed by cessation and inhibition. Both activation and inhibition responses were achieved earlier in the Stx2+L-NAME-treated animals, indicating that NO suppression further enhanced Stx2-mediated platelet activation.

NO inhibition potentiated Stx2-induced platelet degranulation

The previously mentioned data indicated that Stx2 treatment was able to induce platelet activation, as denoted by cell counts and aggregative response, and that inhibition of NO production by L-NAME potentiated this activation. As another marker of platelet activation, platelet intracellular ADP granule content was measured by means of a cytometric technique. First, the mepacrine staining in platelets was evaluated both in controls and Stx2-treated mice at different times after the Stx2 injection. As shown in Figure 7A, a significant reduction in granule content was observed in the Stx2 group at 48 and 72 hours. At this Stx2 concentration, however, no difference could be appreciated between the Stx2 and the Stx2+L-NAME groups (data not shown). To elucidate whether L-NAME pretreatment was able to further enhance Stx2 action, we then used a lower dose of Stx2 (300 pg/mouse), at which Stx2 by itself exerted no effect on platelet degranulation. Results shown in Figure 7B indicate that Stx2+L-NAME-induced degranulation became evident, thus suggesting that L-NAME pretreatment was able to potentiate Stx2-mediated degranulation. Again, the effect of L-NAME was prevented by L-ARG addition. It is worth noting that neither L-NAME

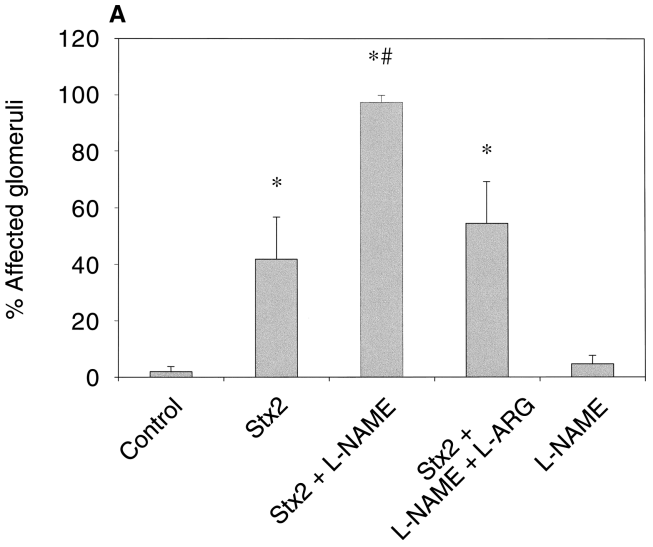

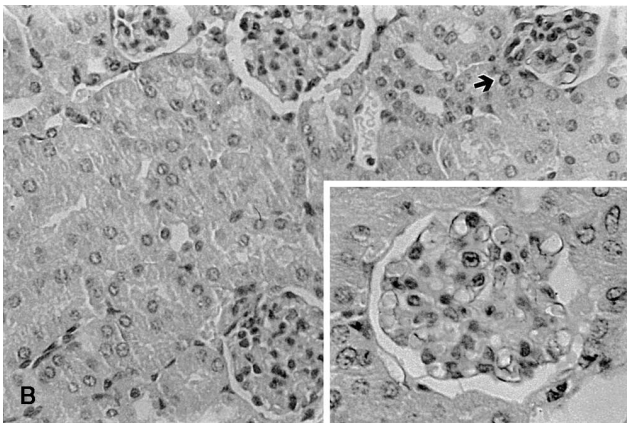

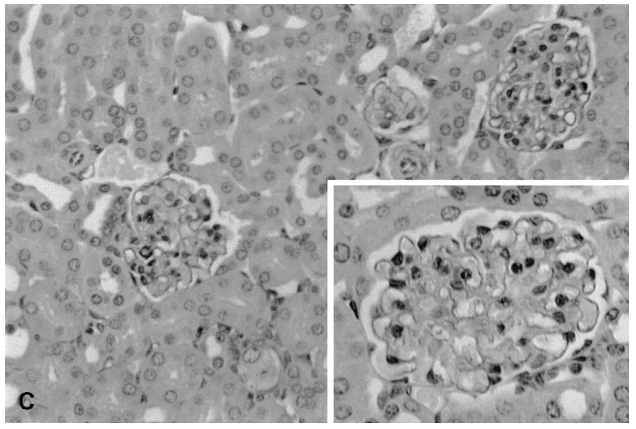

Fig. 5. Immunostaining for fibrinogen. (*A*) A mean number of 100 fields (×40) was counted and the percentage (± SEM) of glomeruli positively stained for fibrinogen was determined for every experimental group (*$P < 0.001$, compared to controls and to L-NAME; #$P < 0.0125$, compared to Stx2 and to Stx2+L-NAME+L-ARG). (*B*) Renal section from Stx2-treated mice, showing 1 out of 4 glomeruli positively stained for fibrinogen (arrow) (×250). The inset shows that the antifibrinogen antibody has specifically detected thrombosis in glomerular capillaries (×400). (*C*) Renal section from Stx2+L-NAME-treated mice, where every glomerulus is positively stained (×250). The insert shows a glomerulus with highly stained material in the vessel wall and occluding the lumen (×400).

Table 1. Alteration in platelet counts induced by Stx2 and L-NAME

Time *hours*	Control	Stx2	Stx2+L-NAME
12	8.46 ± 0.18	13.12 ± 0.67[a]	17.80 ± 0.24[ab]
24	8.66 ± 0.43	6.41 ± 0.35[a]	5.93 ± 0.45[a]
72	8.58 ± 0.66	6.96 ± 0.29[a]	5.51 ± 0.71[a]

Data are expressed as platelet counts × 10^5 per μL (mean ± SEM). Platelet number was determined in platelet rich plasma (PRPs) of control ($N = 5$) and treated ($N = 7$) animals, at different times after Stx2 injection.

[a] $P < 0.01$, compared to controls

[b] $P < 0.02$, compared to Stx2

nor L-ARG by themselves induced any change in platelet activation or degranulation.

Platelet participation in Stx2 and L-NAME action

The involvement of platelets in the effect of Stx2 and Stx2+L-NAME treatments was evaluated in animals in which the platelet population was removed by means of a specific polyclonal antiserum obtained in rabbit. Figure 8 shows that Stx2-mediated mortality was not modified by the absence of platelets. On the contrary, the worsening effect of L-NAME upon Stx2 toxicity was abolished in the platelet depleted mice, suggesting that this effect was mediated, at least in part, by platelets. These results indicate that there is a deleterious basal effect exerted by Stx2 itself that operates independently of platelets; in contrast, this cell population might be involved in the enhancing action of L-NAME, probably through the formation of thrombi.

Stx2 induced the generation of NO metabolites

To evaluate whether Stx2 injection modified the L-ARG-NO pathway activity in the mouse model, NO generation was measured as total NO_2^- plus NO_3^- concentration in sera of control and treated mice, at different times after Stx2 injection. At 12 and 24 hours post-Stx2, no variations were detected in the NO concentration (data not shown). However, at 48 hours, treatment with Stx2 significantly enhanced basal production of NO (Table 2); pretreatment with L-NAME was able to prevent this Stx2-mediated effect. Oral administration of L-NAME

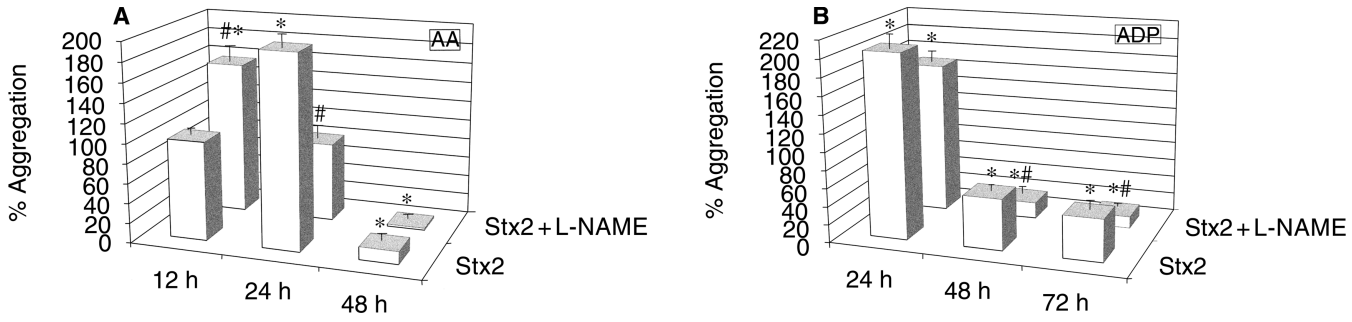

Fig. 6. Platelet aggregative response against (*A*) arachidonic acid (AA) (*B*) or adenosine diphosphate (ADP). Results are from one representative experiment out of five and are expressed as the percentage of aggregation compared to control (100%). Platelet rich plasma (PRP) from controls, Stx2 and Stx2+L-NAME-treated mice were obtained at different times after Stx2 injection and incubated with AA (final concentration: 0.5 mmol/L) or ADP (final concentration: 2.5 μmol/L). $*P < 0.01$, compared to controls; $\#P < 0.05$, compared to Stx2.

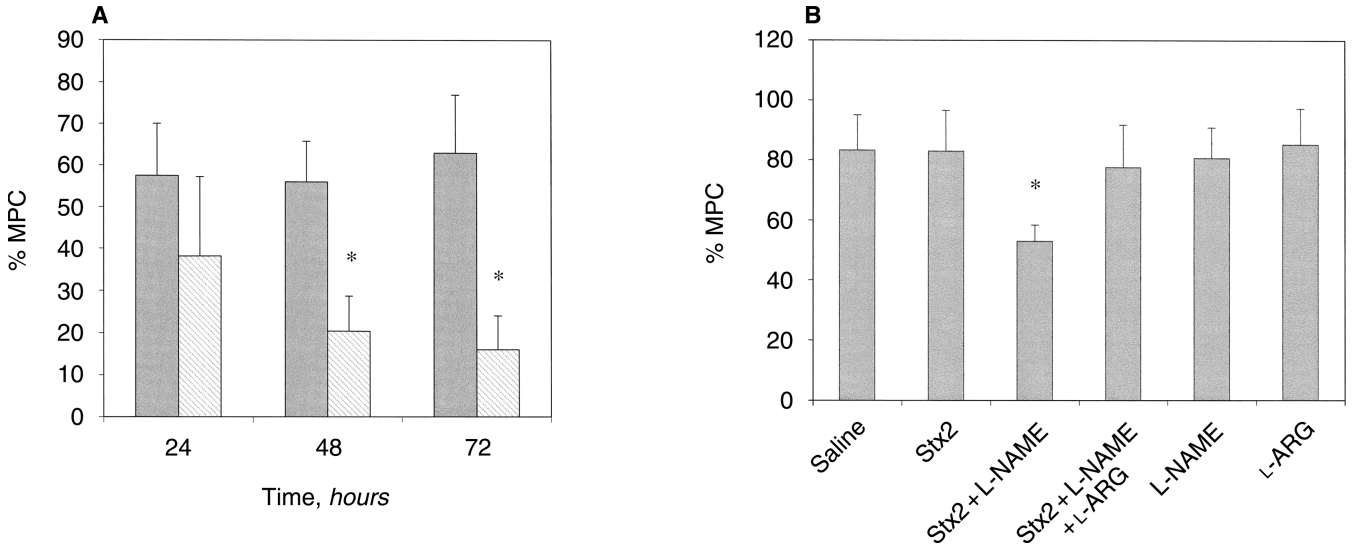

Fig. 7. Mepacrine staining in platelets from Stx2- and Stx2+L-NAME-treated animals (*A*). Symbols are: (▨) saline; (□) Stx2. Mice were bled daily at different times after Stx2 injection (500 pg/mice). Mepacrine staining was determined by flow cytometry. Each bar represents the mean percentage of mepacrine positive cells (% MPC) ± SEM of six mice from one representative experiment out of five ($*P < 0.01$, compared to controls, saline injected animals) (*B*). Percentages of MPC at 48 hours after Stx2 injection (300 pg/mice) corresponding to six mice of a representative experiment out of three ($*P < 0.05$, compared to saline, to Stx2 and to Stx2+L-NAME+L-ARG-treated groups).

at the present concentrations did not cause evident variations in basal serum concentration of NO by itself, in agreement with previous reports [29, 30]. As stated for humans, we were able to detect a late Stx2 induction of NOS activity in mice.

DISCUSSION

Every step in the pathogenic cascade resulting from the invasion of the host by Stx-producing *E. coli* and leads to the final event of microvessel thrombosis in HUS, remains elusive. It has been suggested that platelet activation may be responsible for some of the clinical features. However, the occurrence of platelet hyperactivity has not been demonstrated, probably because it is a very early event. Instead, an impaired platelet function named "platelet exhaustion" has been detected along with thrombocytopenia in most of the hospitalized patients. This impairment consists of a reduced aggregative response, depletion in platelet granule content and shortened platelet survival [6, 8], and is interpreted as the consequence of a prior phase of endothelial damage-induced platelet activation. This concept is supported by many biochemical findings, such as increased plasma levels of platelet derived factors and reduced intraplatelet nucleotides, serotonin and thromboxane A_2 [8, 11, 36–38].

The mouse model used herein allowed an examination of the first stages in the development of HUS and permitted the demonstration that Stx2 induces an early platelet activation, as denoted by a higher cell count, enhanced aggregative response to different agonists and degranulation. This activation is rapidly followed by inhibition,

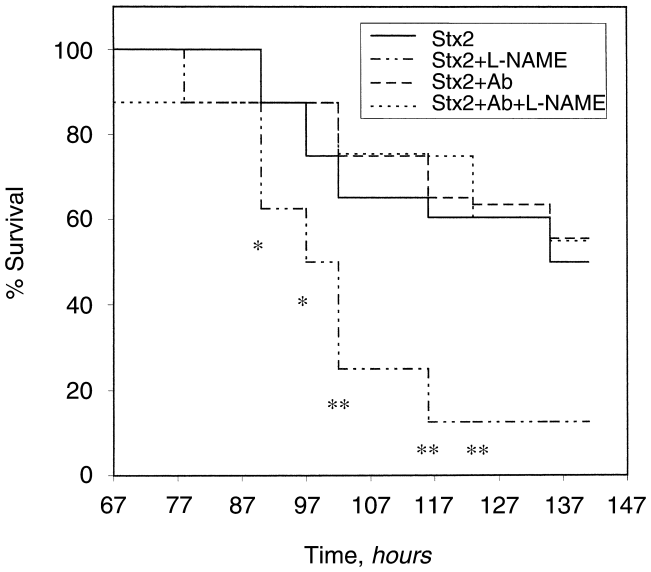

Fig. 8. Stx2 and Stx2+L-NAME lethality in mice depleted from platelets. Groups of six mice were injected with a rabbit polyclonal antiserum against mouse platelets (Ab), to induce significant reduction in platelet number. Then mice received Stx2 or Stx2+L-NAME as detailed before. Pooled survival percentages corresponding to 18 animals are shown (*$P < 0.05$; **$P < 0.01$, compared to Stx2+Ab+L-NAME).

consistent with the platelet exhaustion described in humans. It is noteworthy that the results from the platelet depletion studies indicate that a severe antibody-induced thrombocytopenia does not prevent Stx2 lethality. This suggests that platelet activation constitutes a worsening modulation factor operating within Stx2-induced pathogenicity.

Despite evidence of the activation of NO pathway during HUS [12–14], the actual role of NO in the pathogenesis of the illness is still controversial [11, 13–18]. We investigated the potential pathophysiological role of endogenous NO in Stx2 toxicity by blocking its production by means of NOS inhibitors. The NOS inhibitor L-NAME enhanced Stx2-stimulated renal damage and mortality. Moreover, L-NAME accelerated and amplified the Stx2-induced pattern of platelet activation followed by platelet exhaustion, as assessed by the higher number of circulating platelets, earlier achieved aggregative response and enhanced degranulation. In favor of platelet activation contributing to the pathogenicity of Stx2, it can be postulated that the inhibition of NO synthesis enhances renal damage and leads to death, at least in part, by potentiating the platelet activity and the consequent thrombus formation. In fact, the enhancing effect of L-NAME is not observed in thrombocytopenic mice.

Histological findings strengthen this hypothesis since pretreatment of mice with L-NAME aggravated Stx2-induced renal alterations, and led not only to widespread glomerular thrombosis, but also to extensive necrotic areas

Table 2. Generation of NO metabolites by Stx2

Treatment	$[NO_2]^-$ in serum *mmol/L X ± SEM*	*N*
None	5.1 ± 1.1	12
Stx2	9.4 ± 3.0[a]	12
L-NAME	4.9 ± 0.7[b]	12
Stx2+L-NAME	5.2 ± 2.3[b]	12

Total nitrite concentration ($[NO_2]^-$) was measured in sera of animals treated with Stx2, L-NAME or Stx2+L-NAME, 48 hours after Stx2 injection.
[a] $P < 0.05$
[b] Non-significant, compared to controls

in the proximal and distal tubular epithelium, whereas the addition of L-ARG prevented this effect. On the other hand, kidneys from mice receiving only L-NAME displayed unaltered tubular epithelial architecture, with dilated intraglomerular capillaries and cortical interstitial vascular congestion. It is important to point out that these alterations could be attributed to the vasoactive effect of L-NAME and are unlikely to be responsible per se for the increase in plasmatic urea, renal injury and mortality after L-NAME treatment of Stx2-injected mice. This leads us to postulate that L-NAME–mediated effects reflect a real worsening of renal damage induced by Stx2 instead of a hemodynamic phenomenon.

In the kidney, neuronal NOS in the macula densa and endothelial constitutive NOS (ecNOS) are involved in the regulation of glomerular hemodynamics; in addition there is iNOS, which is specifically activated during inflammation [39]. Since L-NAME is a non-specific NOS inhibitor [40], we tested the effect of two selective iNOS inhibitors, AG and L-NIL. The observation that neither AG (which is 100-fold more potent than L-NAME) nor L-NIL, a highly potent murine iNOS inhibitor [41], exerted any effect on Stx2-induced lethality indicates that the constitutive isoform of NOS would be preferentially involved in the deleterious effect of L-NAME. In summary, these results suggest that cNOS releases NO, which is capable of ameliorating Stx2-induced injury by reducing Stx2-mediated platelet aggregation, raising the possibility that NO could be a physiological regulator for platelet dysfunction and thrombus formation in HUS. This is in agreement with the general concept stating that moderate amounts of NO released by cNOS play a homeostatic role; conversely, high concentrations of NO resulting from the output of iNOS usually lead to tissue injury. In HUS, an excessive NO release has been associated with the secretion of inflammatory mediators (such as TNF-α, IL-1) and the generation of highly cytotoxic radicals [18].

In keeping with our results, beneficial effects of NO have been demonstrated in a rat model for endotoxemia [42], where NO is important in maintaining renal perfusion and preventing endotoxin-induced platelet aggregation and thrombosis in glomeruli during shock [43].

Moreover, experimentally induced glomerular thrombosis in rats was attenuated by treating the animals with exogenous NO donor nitroglycerin [44]. In that model, endothelial cNOS activity accounted for the protective effects of NO [45].

A presumed protective role for NO in HUS also has been theorized by Jaradat and Marquardt [15], who proposed that oral administration of L-arginine could generate NO, which in turn would decrease platelet aggregation and increase vasodilation. To our knowledge, only one experimental protocol exists in which one patient undergoing the acute phase of thrombotic thrombocytopenic purpura (TTP), a disease closely related to HUS, received oral L-arginine and experienced a lower number of relapses [14]. These authors outlined the importance of considering a supply of exogenous L-arginine as an alternative approach to control microangiopathies.

It has been demonstrated that L-arginine inhibits platelet aggregation by its direct action on an intraplatelet constitutive calcium-dependent NOS [46, 47]. The NO generated would additionally inhibit platelet recruitment to the growing thrombus [48]. In our model, L-arginine administration *per se* did not result in improved survival, but only reversed the L-NAME–mediated worsening effect. Since cNOS would be the implicated isoform, which is saturated by physiologic amounts of L-arginine, an excess of additional substrate is not likely to be available to the enzyme.

We also found that Stx2 treatment enhanced basal NO production, in agreement with several reports where NO and NO metabolites were markedly increased in the serum of patients with HUS [12–14]. However, the time course of this increment is delayed compared to Stx2+ L-NAME–mediated action on platelets, and therefore, it is likely to be a late consequence of Stx2-induced pathogenicity. Whether NO overproduction in mice could be attributed to the inducible or the constitutive isoform of the enzyme is not clear, although it can be speculated to be secondary to the endothelial injury and/or the inflammatory response associated with HUS, and thus would probably reflect activation of iNOS.

In conclusion, our results indicate that NO plays a protective role in the early pathogenesis of HUS and emphasize its importance in maintaining the antithrombogenic properties of the endothelium.

ACKNOWLEDGMENTS

This work was supported by grants from Consejo Nacional de Investigaciones Científicas y Técnicas (CONICET) (PIP N° 0597/98), Fundación Alberto J. Roemmers and Agencia Nacional de Promoción Científica y Tecnológica, Argentina. The authors thank Dr. Christiane Dosne Pasqualini for reviewing this manuscript, J. Portaluppi and A. Morales for their technical assistance, and Fundación de la Hemofilia and Academia Nacional de Medicina for the use of the FACScan flow cytometer.

Reprint requests to Dr. Graciela I. Dran, Ph.D., División Medicina Experimental, Instituto de Investigaciones Hematológicas, Academia Nacional de Medicina, Pacheco de Melo 3081, 1425 Capital Federal, República Argentina.
E-mail: colodran@hotmail.com

APPENDIX

Abbreviations used in this article are: AA, arachidonic acid; ADP, adenosine diphosphate; AG, aminoguanidine; CD_{50}, 50% cytotoxic dose; cGMP, cyclic 3′,5′-guanosine monophosphate; D-NAME, D-nitro-L-arginine methyl ester; Gb3, globotriaosil ceramide; *E. coli*, *Escherichia coli*; H&E, hematoxylin and eosin (stain); HPLC, high pressure liquid chromatography; HUS, hemolytic uremic syndrome; iNOS, inducible nitric oxide synthase; IL, interleukin; L-ARG, L-arginine; LD_{50}, lethal dose 50%; L-NAME, L-N^G-nitro-L-arginine methyl ester; L-NIL, L-N^6(1-imino-ethyl)-lysine; NO, nitric oxide; NO_2^-, nitrite; NO_3^-, nitrate; NOS, nitric oxide synthase; PAS, periodic acid Schiff (stain); PGI_2, prostacyclin; PPP, platelet poor plasma; PRP, platelet rich plasma; Stx2, Shiga toxin 2; TMA, thrombotic microangiopathy; TNFα, tumor necrosis factor-α; TTP, thrombocytopenic purpura.

REFERENCES

1. Riley LW, Remis RS, Helgerson SD, *et al*: Hemorrhagic colitis associated with a rare *Escherichia coli* O157:H7 serotype. *N Engl J Med* 308:681–685, 1983
2. Gordjani N, Sutor AH, Zimmerhackl LB, Brandis M: Hemolytic uremic syndrome in childhood. *Semin Thromb Hemost* 23: 281–293, 1997
3. Milford DV, Taylor CM, Rafaat F, Halloran E: Neutrophil elastases and haemolytic uremic syndrome. *Lancet* 11:1153, 1989
4. Richardson SE, Karmali MA, Becker LE, Smith CR: The histopathology of the hemolytic uremic syndrome associated with verocytotoxin-producing *Escherichia coli* infections. *Hum Pathol* 19: 1102–1108, 1988
5. Siegler RL: Spectrum of extrarenal involvement in postdiarrheal hemolytic-uremic syndrome. *J Pediatr* 125:511–518, 1994
6. Fong JSC, Kaplan BS: Impairment of platelet aggregation in hemolytic uremic syndrome: Evidence for platelet "exhaustion." *Blood* 60:564–570, 1982
7. Lian ECY: Pathogenesis of thrombotic thrombocytopenic purpura. *Semin Hematol* 24:82–100, 1987
8. Walters MDS, Levin M, Smith C, *et al*: Intravascular platelet activation in the hemolytic uremic syndrome. *Kidney Int* 33:107–115, 1988
9. Moncada S, Palmer RM, Higgs EA: Nitric oxide: Physiology, pathophysiology and pharmacology. *Pharmacol Rev* 43:109–142, 1991
10. Radomski M, Palmer RM, Moncada S: The role of nitric oxide and cGMP in platelet adhesion to vascular endothelium. *Biochem Biophys Res Commun* 148:1482–1489, 1987
11. Noris M, Remuzzi G: Uremic bleeding: Closing the circle after 30 years of controversies? *Blood* 94:2569–2574, 1999
12. Dedeoglu IO, Feld LG: Nitric oxide in the urine of a patient with hemolytic uremic syndrome. *Pediatr Nephrol* 10:812–813, 1996
13. Noris M, Ruggenenti P, Todeschini M, *et al*: Increased nitric oxide formation in recurrent thrombotic microangiopathies: A possible mediator of microvascular injury. *Am J Kidney Dis* 27:790–796, 1996
14. Herlitz H, Petersson A, Sigstrom L, *et al*: The arginine-nitric oxide pathway in thrombotic microangiopathy. *Scand J Urol Nephrol* 31:477–479, 1997
15. Jaradat ZW, Marquardt RR: L-arginine as a therapeutic approach for the verotoxigenic *Escherichia coli*-induced hemolytic uremic syndrome and thrombotic thrombocytopenic purpura. *Med Hypotheses* 49:277–280, 1997
16. Mulligan MS, Hevel JM, Marletta MA, Ward PA: Tissue injury caused by deposition of immune complexes is L-arginine dependent. *Proc Natl Acad Sci USA* 88:6338–6342, 1991
17. Estrada C, Gomez C, Martin C, *et al*: Nitric oxide mediates tumor necrosis factor alpha cytotoxicity in endothelial cells. *Biochem Biophys Res Commun* 186:475–482, 1992

18. Remuzzi G, Ruggenenti P: The hemolytic uremic syndrome. *Kidney Int* 53:54–57, 1998
19. Beery JT, Doyle MP, Higley NA: Cytotoxic activity of *Escherichia coli* 0157:H7 culture filtrate on the mouse colon and kidney. *Curr Microbiol* 11:335–342, 1984
20. Barrett TJ, Potter ME, Wachsmuth IK: Continuous peritoneal infusion of Shiga-like toxin-II (SLT-II) as a model for SLT-II-induced diseases. *J Infect Dis* 159:774–777, 1989
21. Wadolkowski EA, Burris J, O'Brien AD: Mouse model for colonization and disease caused by enterohemorrhagic *Escherichia coli* O157:H7. *Infect Immun* 58:2438–2445, 1990
22. Wadolkowski EA, Sung LM, Burris J, *et al*: Acute renal tubular necrosis and death of mice orally infected with *Escherichia coli* strains that produce Shiga-like toxin type II. *Infect Immun* 58:3959–3965, 1990
23. Tesh VL, Burris JA, Owens JW, *et al*: Comparison of the relative toxicities of Shiga-like toxins type I and II for mice. *Infect Immun* 61:3392–3402, 1993
24. Harel Y, Silva M, Giroir B, *et al*: A reporter transgene indicates renal-specific induction of tumor necrosis factor (TNF) by Shiga-like toxin. *J Clin Invest* 92:2110–2116, 1993
25. Karpman D, Connell H, Svensson M, *et al*: The role of lipopolysaccharide and Shiga-like toxin in a mouse model of *Escherichia coli* O157:H7 infection. *J Infect Dis* 175:611–620, 1997
26. Palermo MS, Alves Rosa MF, Van Rooijen N, Isturiz MA: Depletion of liver and splenic macrophages reduces the lethality of Shiga toxin-2 in a mouse model. *Clin Exp Immunol* 116:462–467, 1999
27. Palermo MS, Alves Rosa MF, Rubel C, *et al*: Pretreatment of mice with lipopolysaccharide (LPS) or IL-1 exerts dose-dependent opposite effects on Shiga toxin-2 lethality. *Clin Exp Immunol* 119: 77–83, 2000
28. Karmali MA, Petric M, Lim C, *et al*: The association between idiopathic uremic syndrome and infection by verotoxin-producing *Escherichia coli. J Infect Dis* 151:775–782, 1985
29. Arnal JF, Munzel T, Venema RC, *et al*: Interactions between L-arginine and L-glutamine change endothelial NO production. *J Clin Invest* 95:2565–2572, 1995
30. Orucevic A, Lala PK: N-nitro-L-arginine methyl ester, an inhibitor of nitric oxide synthesis, ameliorates interleukin 2-induced capillary leakage and reduces tumor growth in adenocarcinoma-bearing mice. *Br J Cancer* 73:189–196, 1996
31. Ehlers S, Kutsch S, Benini J, *et al*: NOS2-derived nitric oxide regulates the size, quantity and quality of granuloma formation in Mycobacterium avium-infected mice without affecting bacterial loads. *Immunology* 98:313–323, 1999
32. Vermeire K, Thielemans L, Matthys P, Billiau A: The effects of NO synthase inhibitors on murine collagen-induced arthritis do not support a role of NO in the protective effect of IFN-gamma. *J Leukoc Biol* 68:119–124, 2000
33. Gordon N, Thom J, Cole C, Baker R: Rapid detection of hereditary and acquired platelet storage pool deficiency by flow cytometry. *Br J Haematol* 89:117–123, 1995
34. Zhou XJ, Laszik Z, Ni Z, *et al*: Down-regulation of renal endothelial nitric oxide synthase expression in experimental glomerular thrombotic microangiopathy. *Lab Invest* 80:1079–1087, 2000
35. Heeringa P, van Goor H, Lindstrom YI, *et al*: Lack of endothelial nitric oxide synthase aggravates murine accelerated anti-glomerular basement membrane glomerulonephritis. *Am J Pathol* 156:879–888, 2000
36. Pareti FI, Capitanio A, Mannucci L, *et al*: Acquired dysfunction due to the circulation of exhausted platelets. *Am J Med* 69:235–240, 1980
37. Edefonti A, Bettinelli A, Mondonico P, *et al*: Intraplatelet serotonin in children with hemolytic uremic syndrome. *Clin Nephrol* 23:207–211, 1985
38. Tonshoff B, Momper R, Gonne Kuhl P, *et al*: Increased thromboxane biosynthesis in childhood hemolytic uremic syndrome. *Kidney Int* 37:1134–1141, 1990
39. Ketteler M, Abou-Rebyeh F, Frey A, *et al*: Nitric oxide, L-arginine and the kidney. Experimental studies of new therapy approaches. *Med Klin* 93:15–21, 1998
40. Miller MJS, Clark DA: Nitric oxide synthase inhibition can initiate or prevent gut inflammation: role of enzyme source. *Agents Actions* 41:C231–C232, 1994
41. Moore WM, Webber RK, Jerome GM, *et al*: L-N6-(1-iminoethyl)-lysine: A selective inhibitor of inducible nitric oxide synthase. *J Med Chem* 37:3886–3888, 1994
42. Vedanarayanan VV, Kaplan BS, Fong JSC: Neutrophil function in an experimental model of hemolytic uremic syndrome. *Pediatr Res* 21:252–256, 1987
43. Shultz PJ, Raij L: Endogenously synthesized nitric oxide prevents endotoxin-induced glomerular thrombosis. *J Clin Invest* 90:1718–1725, 1992
44. Westberg G, Shultz PJ, Raij L: Exogenous nitric oxide prevents endotoxin-induced glomerular thrombosis in rats. *Kidney Int* 46: 711–716, 1994
45. Shao J, Miyata T, Yamada K, *et al*: Protective role of nitric oxide in a model of thrombotic microangiopathy in rats. *J Am Soc Nephrol* 12:2088–2097, 2001
46. Marietta M, Facchinetti F, Neri I, *et al*: L-arginine infusion decreases platelet aggregation through an intraplatelet nitric oxide release. *Thromb Res* 88:229–235, 1997
47. Diodati JG, Nader D, Gilligan DM, Quyyumi A: Effect of atherosclerosis on endothelium-dependent inhibition of platelet activation in humans. *Circulation* 98:17–24, 1998
48. Freedman JE, Loscalzo J, Barnard MR, *et al*: Nitric oxide released from activated platelets inhibits platelet recruitment. *J Clin Invest* 100:350–356, 1997